

Flow of Nucleons and Fragments in $^{40}\text{Ar} + ^{27}\text{Al}$ Collisions Studied with AMD

Akira Ono and Hisashi Horiuchi

Department of Physics, Kyoto University, Kyoto 606-01, Japan

Abstract

Collective transverse momentum flow of nucleons and fragments in intermediate energy $^{40}\text{Ar} + ^{27}\text{Al}$ collisions is calculated with the antisymmetrized molecular dynamics (AMD). The observed flow and its balance energy are reproduced very well by the calculation with the Gogny force which corresponds to the soft EOS of the nuclear matter. Especially the calculated absolute value of the fragment flow is larger than that of the nucleon flow in the negative flow region, which can be explained by the existence of two components of flow. In addition to many similarities, difference in the deuteron flow is found between $^{12}\text{C} + ^{12}\text{C}$ and $^{40}\text{Ar} + ^{27}\text{Al}$ collisions, and its origin is investigated by paying attention to the production mechanism of light fragments. We also investigate the dependence of the flow of nucleons and fragments on the stochastic collision cross section and the effective interaction, and conclude that the stiff EOS without momentum dependence of the mean field is not consistent to the experimental data.

I. INTRODUCTION

In intermediate and high energy heavy ion collisions, high density and high temperature region is created, and the collective flow in heavy ion reactions has been studied in order to extract the information on the hot and dense nuclear matter. Since the relevant energy scale such as the compression energy per nucleon and the depth of the nuclear mean field is several tens MeV, we can expect that intermediate energy heavy ion collisions with the incident energy region from several tens MeV/nucleon up to a few hundreds MeV/nucleon are suitable for the above mentioned purpose. At lower incident energy in this energy region, the attractive (negative) flow pattern is produced due to the attractive interaction between projectile and target nuclei. And above a certain incident energy, called balance energy, the flow changes into repulsive (positive) by the effects of more two-nucleon collisions, higher compression and the momentum dependence of the mean field. This balance energy has been paid attention to as a good indicator of the equation of state (EOS) of the nuclear matter, but by the study with microscopic simulation approaches such as Vlasov-Uehling-Uhlenbeck method, it has turned out that extracting the EOS is not easy since the inclusive collective flow reflects not only the EOS but also other factors such as the cross section of the two-nucleon collision term which has theoretical ambiguity in the nuclear medium.

Although the collective flow is usually considered as a one-body observable, the most characteristic feature of intermediate energy heavy ion reactions is the fragment formation. Recently the collective flow has become to be measured exclusively with the identification of charges and/or mass numbers of fragments [1–5]. The observed flow of fragments has been found to be large compared to the flow of nucleons. The reason is that most nucleons are emitted by the hard stochastic collisions which erase largely the effect of the mean field in the nucleon flow. It suggests that the flow of composite fragments carries precious information on the EOS (or the mean field). In our previous work on $^{12}\text{C} + ^{12}\text{C}$ collisions, we found that the flow in the incident energy region of negative flow consists of two components at the end of the dynamical stage of the reaction, i.e., the flow of nucleons emitted by stochastic collisions and the flow of excited fragments or the nuclear matter which is largely affected by the mean field. Thus we can expect that the systematic study of the fragment flow together with the nucleon flow may give us important information on the EOS.

For the theoretical analysis of the flow of fragments, the model should be able to describe the dynamical fragment formation, and we use the antisymmetrized molecular dynamics with stochastic collisions (AMD) [6–12]. In AMD, the system is described with a Slater determinant of Gaussian wave packets and the time development of the centers of the wave packets is determined by the time dependent variational principle and the stochastic collision process. We have demonstrated that the AMD can describe some quantum mechanical features such as the shell effect in the dynamical production of fragments in the intermediate energy heavy ion reactions. Furthermore, since we use the antisymmetrized wave function in AMD, the ground states of initial nuclei are the most precisely described among many simulation methods for heavy ion reactions and have no ambiguity in the choice of them because the ground states are the states which give the minimum value of the Hamiltonian with an effective interaction. By using a finite range effective interaction such as the Gogny force, the momentum dependence of the mean field is automatically taken into account.

In this paper, we calculate $^{40}\text{Ar} + ^{27}\text{Al}$ collisions with AMD in the incident energy region

25 MeV $\leq E/A \leq$ 135 MeV and analyze the collective transverse momentum flow of nucleons and fragments as well as other features of their momentum distribution. The purpose of this paper is two fold. One is to get understanding on the production mechanism of the flow of nucleons and fragments. It is very important to understand the reaction mechanism before getting anything from heavy ion reactions. We will really see that the production mechanism of light fragments such as deuterons and α particles is closely related to their flow by comparing the present results with our previous results for $^{12}\text{C} + ^{12}\text{C}$ collisions [9]. The second purpose is to investigate the dependence of the flow on the two-nucleon collision cross section and on the effective interaction, based on which we discuss the determination of the EOS of the nuclear matter. We make calculations with Gogny force which gives the soft EOS of the nuclear matter and momentum dependent mean field and with a kind of Skyrme force (called SKG2 in this paper) which gives stiff EOS and mean field with little momentum dependence. It will be concluded that the Gogny force reproduce the observed data very well while the SKG2 force does not, in spite of some ambiguity of the stochastic collision cross section.

This paper is organized as follows. After explaining the outline of the framework briefly in Sec. II, some calculated quantities such as mass distribution and momentum distribution of produced fragments are presented in Sec. III in order to show the overall features of the reaction investigated in this paper. In Sec. IV, the calculated results of the flow of nucleons and fragments with the Gogny force are discussed, and in Sec. V the flow of light fragments such as deuterons is investigated by paying attention to their production mechanism and comparing it with the case of $^{12}\text{C} + ^{12}\text{C}$ collisions. The dependence of the results on the stochastic collision cross section and on the adopted effective interaction is discussed in Sec. VI in order to determine the EOS. Section VII is devoted to the summary.

II. OUTLINE OF THE METHOD

Since the framework of the antisymmetrized version of molecular dynamics (AMD) was described in detail in Refs. [7–9], here is shown only the outline of our framework.

In AMD, the wave function of A -nucleon system is described by a Slater determinant $|\Phi(Z)\rangle$,

$$|\Phi(Z)\rangle = \frac{1}{\sqrt{A!}} \det[\varphi_i(j)], \quad \varphi_i = \phi_{\mathbf{Z}_i} \chi_{\alpha_i}, \quad (1)$$

where α_i represents the spin-isospin label of i th single particle state, $\alpha_i = \text{p } \uparrow, \text{p } \downarrow, \text{n } \uparrow, \text{ or } \text{n } \downarrow$, and χ is the spin-isospin wave function. $\phi_{\mathbf{Z}_i}$ is the spatial wave function of i th single particle state which is a Gaussian wave packet

$$\langle \mathbf{r} | \phi_{\mathbf{Z}_i} \rangle = \left(\frac{2\nu}{\pi} \right)^{3/4} \exp \left[-\nu \left(\mathbf{r} - \frac{\mathbf{Z}_i}{\sqrt{\nu}} \right)^2 + \frac{1}{2} \mathbf{Z}_i^2 \right], \quad (2)$$

where the width parameter ν is treated as time-independent in our model. We took $\nu = 0.16 \text{ fm}^{-2}$ in the calculation presented in this paper.

The time developments of the centers of Gaussian wave packets, $Z = \{\mathbf{Z}_i \text{ (} i = 1, 2, \dots, A \text{)}\}$, are determined by two processes. One is the time development determined by the time-dependent variational principle

$$\delta \int_{t_1}^{t_2} dt \frac{\langle \Phi(Z) | (i\hbar \frac{d}{dt} - H) | \Phi(Z) \rangle}{\langle \Phi(Z) | \Phi(Z) \rangle} = 0, \quad (3)$$

which leads to the equation of motion for Z .

The second process which determines the time development of the system is the stochastic collision process due to the residual interaction. We incorporate this process in the similar way to the quantum molecular dynamics (QMD) by introducing the physical coordinates $\{\mathbf{W}_i\}$ [6,7] as

$$\mathbf{W}_i = \sum_{j=1}^A (\sqrt{Q})_{ij} \mathbf{Z}_j, \quad Q_{ij} = \frac{\partial}{\partial(\mathbf{Z}_i^* \cdot \mathbf{Z}_j)} \log \langle \Phi(Z) | \Phi(Z) \rangle. \quad (4)$$

We use the same energy and density dependent two-nucleon collision cross section as in our previous work [9] which is based on the free cross section of pp and pn scattering and has some reduction in the nuclear medium. The detail is explained in the Appendix B of Ref. [9]. Nucleon-alpha collisions are switched off in the calculation of $^{40}\text{Ar} + ^{27}\text{Al}$ collisions in this paper.

The simulations of AMD are truncated at a finite time $t = t_{\text{sw}}$ ($t_{\text{sw}} = 150$ fm/c in most calculations presented in this paper and $t_{\text{sw}} = 225$ fm/c when incident energy is lower than 30 MeV/nucleon). The dynamical stage of the reaction has finished by this time and some excited fragments have been formed which will emit lighter particles with a long time scale. Such statistical decays of the equilibrated fragments are calculated with a code of Ref. [15] which is similar to the code of Pühlhofer [16].

One of the most important inputs in the study of the collective flow is the choice of the effective interaction. The required property of the effective interaction for the study of flow is that it should reproduce the saturation of the nuclear matter and the bulk properties of nuclei in wide mass number region within the framework of AMD. In this paper we execute calculations with two effective interactions which give different stiffness of the nuclear matter, aiming to determine the EOS by the comparison to the data of flow. The first one is the Gogny force [13] which is composed of the finite range two-body force and the density dependent zero range repulsive force. This force gives a soft EOS of the nuclear matter with the incompressibility $K = 228$ MeV, and also it gives momentum dependent mean field which reproduce the observed energy dependence of the nucleon optical potential depth up to the incident energy 200 MeV/nucleon. The second effective interaction used here is a Skyrme-type interaction. Just for the convenience of the numerical calculation we use a modified version of the effective interaction used in Ref. [14], which has the form

$$v(\mathbf{r}_i, \mathbf{r}_j) = v_0((1 - m) - mP_\sigma P_\tau) \exp[-(\mathbf{r}_i - \mathbf{r}_j)^2/\mu^2] + \frac{t_\rho}{6}(W_\rho + B_\rho P_\sigma - H_\rho P_\tau - M_\rho P_\sigma P_\tau)\rho(\mathbf{r}_i)\delta(\mathbf{r}_i - \mathbf{r}_j), \quad (5)$$

where P_σ and P_τ are the spin and isospin exchange operators respectively. We call this interaction SKG2 force and the parameters are listed in Table I. This force gives similar property of Skyrme VII force; namely stiff EOS of nuclear matter with the incompressibility $K = 373$ MeV and no momentum dependence of the mean field. We have modified the density dependent part from Ref. [14] so that the reasonable symmetry energy is obtained. Without

TABLE I. Parameters of SKG2 force in Eq. (5).

v_0 [MeV]	m	μ [fm]	t_ρ [MeV fm ⁶]	W_ρ	B_ρ	H_ρ	M_ρ
-624.46	0.2	0.68	17269.8	1.0	0.2	-0.8	0.0

TABLE II. Parameters concerned with the subtraction of spurious zero-point oscillations of fragments. Parameters which are used with the Gogny force and SKG2 force in this paper are shown. See Appendix C of Ref. [9] for detail.

Force	ξ	a	$\hat{\xi}$	\hat{a}	$\bar{\xi}$	\bar{a}	g_0	σ	M	T_0 [MeV]
Gogny	2.0	0.6	2.0	0.2	1.0	0.5	1.0	2.0	12.0	9.2
SKG2	2.0	0.6	2.0	0.2	—	—	—	—	—	9.0

this modification, we found that many neutron-rich fragments are produced unphysically in heavy ion collisions.

Since in AMD the center-of-mass motion of the fragment is described by a Gaussian wave packet, we have to subtract from the AMD Hamiltonian $\langle \Phi(Z) | H | \Phi(Z) \rangle / \langle \Phi(Z) | \Phi(Z) \rangle$ the sum of the spurious zero-point energies of the fragments whose number changes with time [7]. The prescription to deal with this problem is given in the appendix C of Ref. [9], and the adopted parameters which are used with Gogny force and SKG2 force are listed in Table II.

In Table III, we show the the ground states of ⁴⁰Ar and ²⁷Al nuclei which are obtained by the frictional cooling method in AMD and used as the initial states of AMD simulations. Both the Gogny force and the SKG2 force give similar ground states with appropriate binding energies. The ground state of ⁴⁰Ar is almost spherical but the obtained ²⁷Al ground state is prolately deformed with $\beta \sim 0.4$. Here the deformation parameters β and γ are defined by

$$t_i = \sqrt{\frac{5}{4\pi}} \beta \cos\left(\gamma - \frac{2\pi}{3}i\right) \quad \text{for } i = 1, 2, 3, \quad (6)$$

where $e^{2t_1} : e^{2t_2} : e^{2t_3}$ is the ratio of eigenvalues of the inertia tensor $\langle r_i r_j \rangle$ with $t_1 + t_2 + t_3 = 0$ and $t_1 \leq t_2 \leq t_3$.

TABLE III. Properties of ground states which are obtained by the frictional cooling method and used as the initial states of AMD simulations. There are shown binding energy, root mean square radius, quadrapole deformation parameters β and γ .

Nucleus	Force	B.E. [MeV]	$\sqrt{\langle r^2 \rangle}$ [fm]	β	γ
⁴⁰ Ar	Gogny	335	3.35	0.16	$< 10^\circ$
	SKG2	340	3.36	0.09	35°
	exp.	344			
²⁷ Al	Gogny	220	3.17	0.40	$< 2^\circ$
	SKG2	225	3.19	0.42	$< 2^\circ$
	exp.	225			

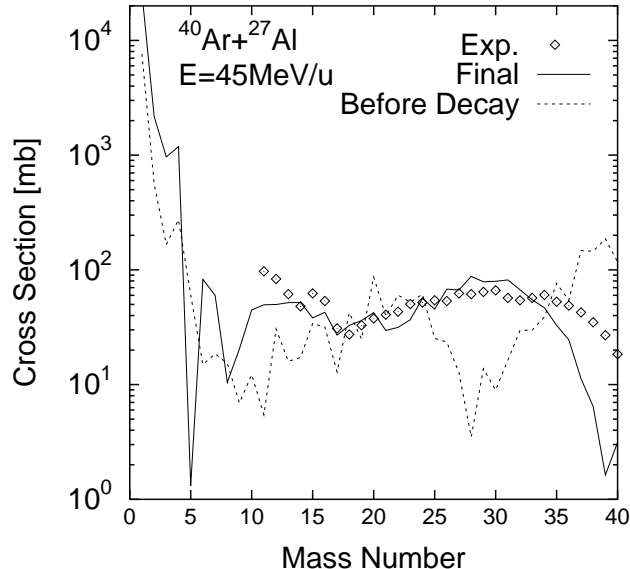


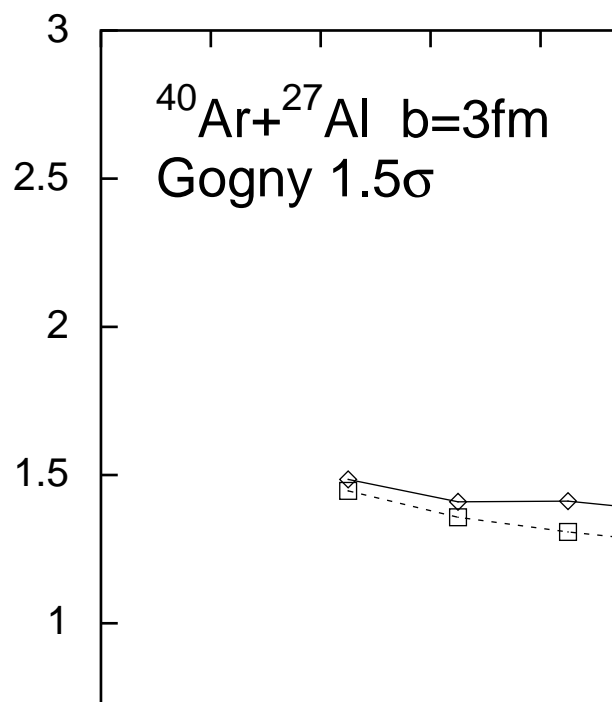
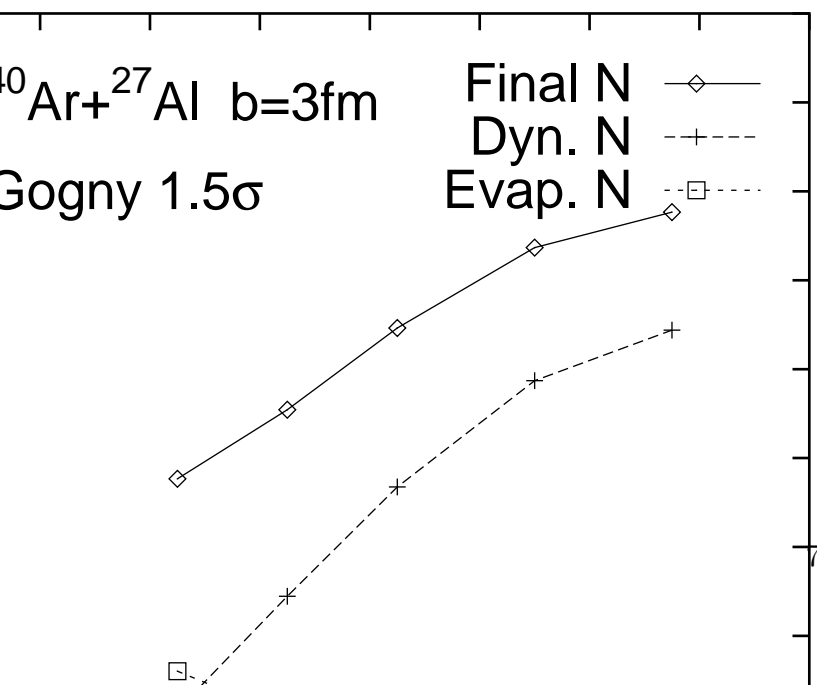
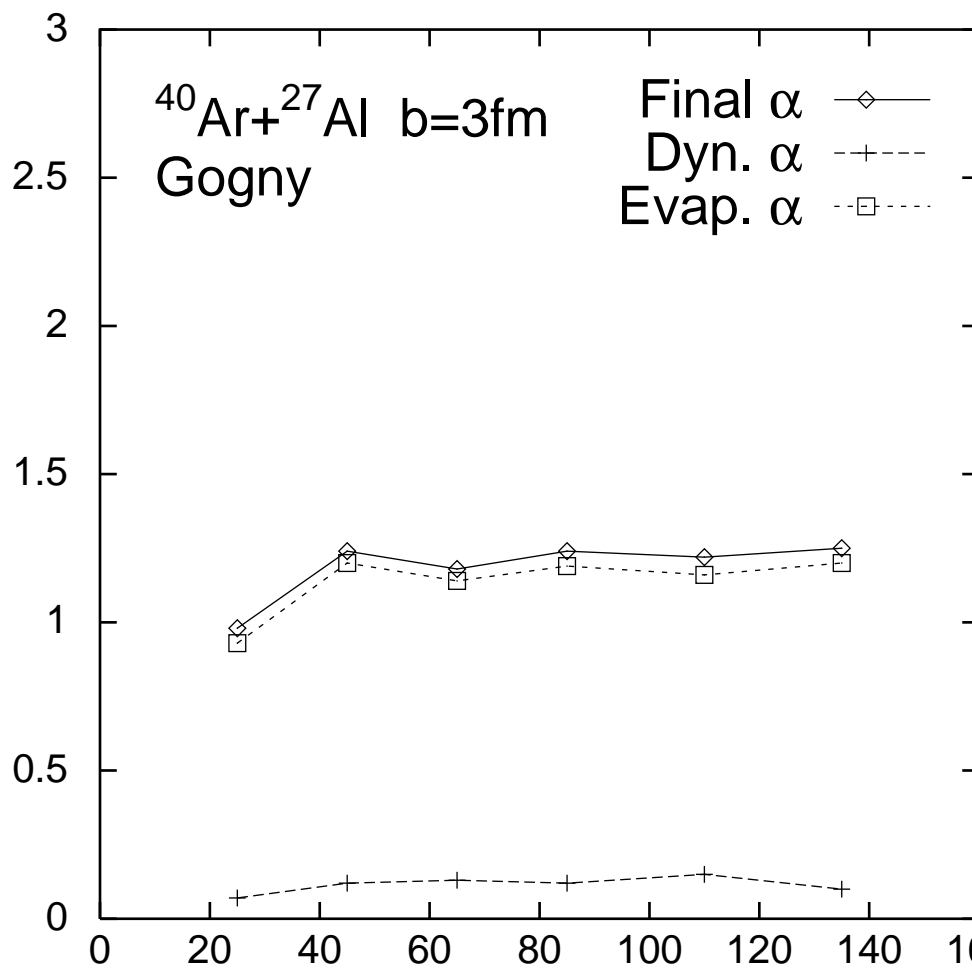
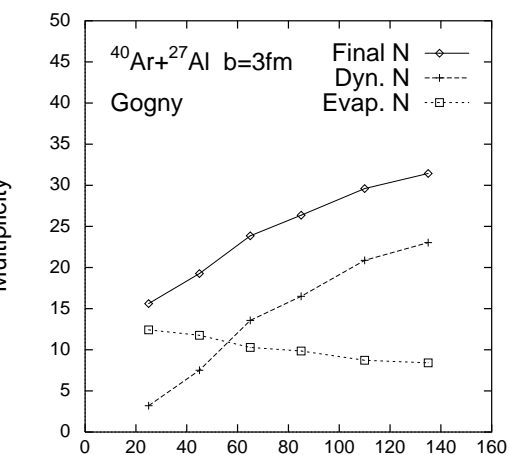
FIG. 1. Mass distribution of fragments in $^{40}\text{Ar} + ^{27}\text{Al}$ reaction at 45 MeV/nucleon. Calculated result at the end of the AMD simulation before the statistical decay is shown by dashed line as well as the final calculated result by solid line. Gogny force was used as the effective interaction. Fragments which are emitted with the angle $\theta > 5^\circ$ and the energy $E/A > 3$ MeV are taken into calculation. Diamonds are the experimental data by Dayras et al. [17] for $^{40}\text{Ar} + ^{27}\text{Al}$ at 44 MeV/nucleon.

III. OVERALL FEATURES OF THE REACTIONS

We have calculated the $^{40}\text{Ar} + ^{27}\text{Al}$ collisions with the incident energy $25 \text{ MeV} \leq E/A \leq 135 \text{ MeV}$. In order to see the overall features of the reaction in this energy region, we will show some calculated quantities with Gogny force in this section.

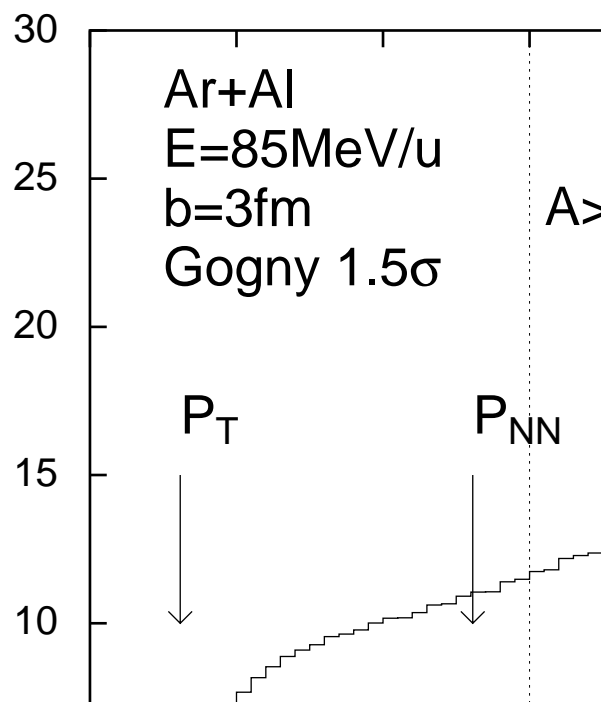
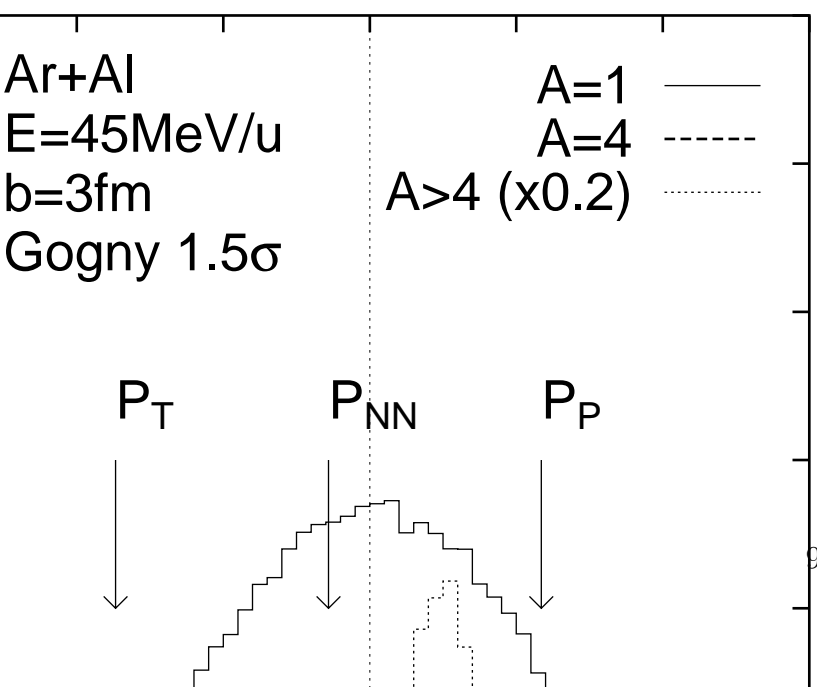
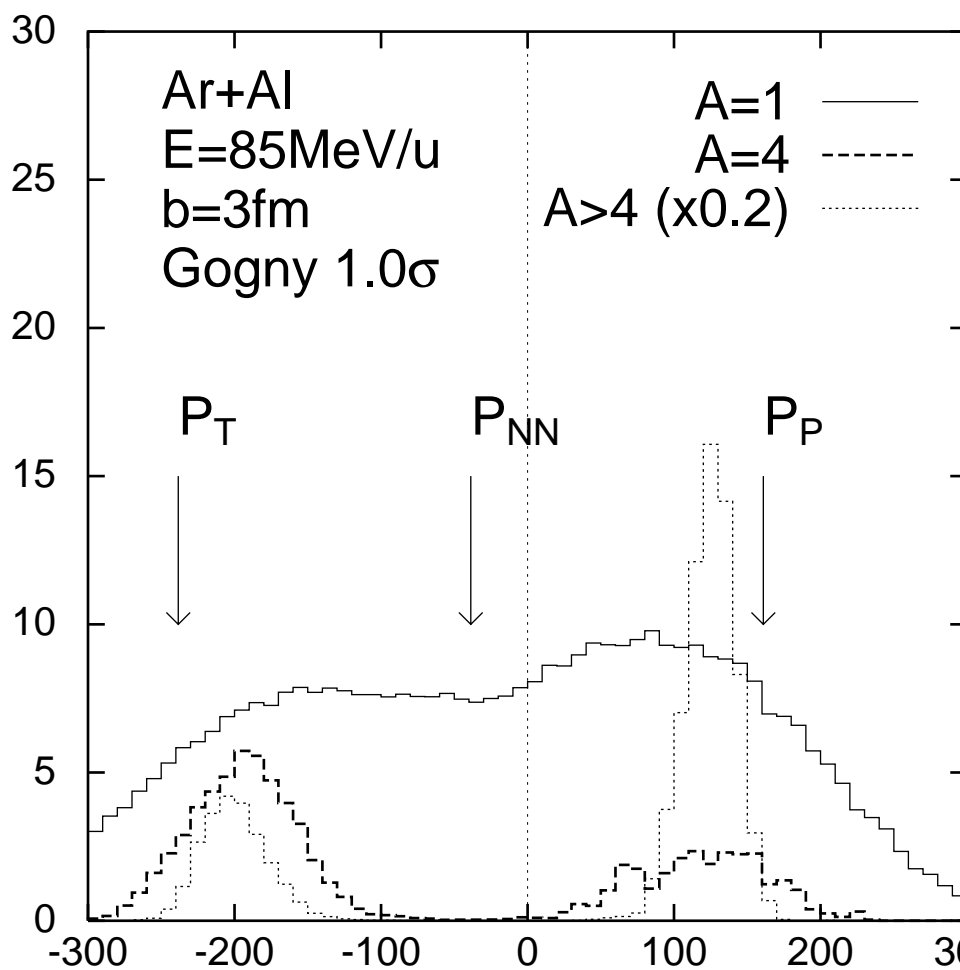
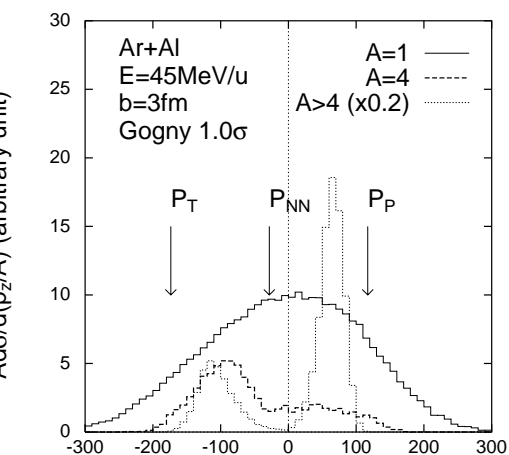
Figure 1 shows the calculated mass distribution of produced fragments at the incident energy 45 MeV/nucleon compared with the experimental data of $^{40}\text{Ar} + ^{27}\text{Al}$ collisions at 44 MeV/nucleon by Dayras et al. [17]. Dashed line shows the mass distribution at $t = t_{\text{sw}}$, namely the result of AMD simulation before the statistical cascade decay, and the solid line shows the final result after the calculation of the statistical cascade decay. In the calculation, we have included only the fragments which are emitted with angles $\theta > 5^\circ$ in the laboratory frame, and the calculated result depends on this threshold angle in the mass number region $A \gtrsim 25$. It can be seen that the observed mass distribution is reproduced as the results of the statistical decay of projectile-like and target-like fragments. It should be noted that the shell effect in the dynamical stage of the reaction has appeared in the large yield of $A = 4$ fragment before the statistical decay but the statistical accuracy is not sufficient in heavier mass number region to discuss the shell effect. The present result of AMD is quite similar to the result of QMD in Ref. [15] in the mass number region $A > 5$.

In Fig. 2, the multiplicities of nucleons and α particles are shown as functions of the incident energy. We fix the impact parameter to 3 fm here and in the following. In addition to



the final multiplicities, there are shown the multiplicities of dynamically produced particles which existed at $t = t_{\text{sw}}$ and the multiplicities of evaporated particles in the statistical decay process. One should keep in mind that the dynamical stage of the reaction has already finished at $t = t_{\text{sw}}$, and therefore the ‘dynamically produced’ particles defined here include some particles *evaporated* from excited fragments which have reached the equilibration before $t = t_{\text{sw}}$. However the main part of the ‘dynamically produced’ particles have been produced before the equilibration. In the calculation of lower two figures, we have increased the stochastic two-nucleon collision cross section by a factor 1.5 (denoted by 1.5σ for simplicity) compared to the calculation of upper two figures where we use the standard cross section (1.0σ) parameterized in the Appendix B of Ref. [9]. As can be expected, the nucleon multiplicity, especially the multiplicity of dynamically emitted nucleons, increases as the incident energy. With 1.0σ , about a quarter of total nucleons are emitted as single nucleons at 25 MeV/nucleon, while this ratio is about a half at 135 MeV/nucleon. On the other hand, the multiplicity of α particles is almost independent of the incident energy in the energy region investigated here. The features of nucleon multiplicity are similar to what we observed in the calculation $^{12}\text{C} + ^{12}\text{C}$ in Ref. [9]. On the contrary, the multiplicity of dynamically produced α particle is much smaller than in $^{12}\text{C} + ^{12}\text{C}$ collisions with $b = 2$ fm where it was about one dynamical α particle per event. This suggests that light nuclei break more easily into small fragments than heavy nuclei. As the two-nucleon collision cross section is increased from 1.0σ to 1.5σ , the dynamical α multiplicity increases as well as the dynamical nucleon multiplicity.

In Fig. 3, the parallel momentum spectra of nucleons and fragments in the collisions with the impact parameter 3 fm are shown for two incident energies 45 MeV/nucleon and 85 MeV/nucleon. The results with 1.0σ and 1.5σ are shown in upper part and in lower part, respectively. Since the center-of-mass motions of fragments are described with wave packets of Gaussian form with the standard deviation $\hbar\sqrt{\nu}/\sqrt{A_F}$ in their momenta per nucleon, we have assumed that the fragments with mass number A_F produced by AMD simulations before the statistical decay have some width in the momentum distribution. Taking account of the fact that part of the width comes from the unphysical width of the initial momenta of the projectile and the target especially for heavy fragments [9], we have attributed the width $\hbar\sqrt{\nu}/A_F$ to their momenta per nucleon. It is clearly seen that there are projectile-like and target-like components in the momentum distribution of heavy fragments, while there is a large component in the nucleon spectrum centered around the center-of-mass velocity of two nucleons in projectile and target (P_{NN} in figures) or the total center-of-mass velocity. As for α particles, there is some yield around the center-of-mass velocity at 45 MeV/nucleon but projectile-like and target-like components clearly separate from each other at 85 MeV/nucleon without any component left around the center-of-mass velocity. More α particles and less heavier fragments are produced in target-like momentum region than in projectile-like momentum region, which means the target nucleus ^{27}Al breaks up into smaller pieces compared to the projectile nucleus ^{40}Ar . The effect of the change of the stochastic collision cross section can be seen in the these spectra. In addition to the yield of nucleons and fragments, the peak position of projectile-like and target-like components are sensitive to the cross section. The peak position of the projectile-like components calculated with the stochastic collision cross section around the investigated value 1.0σ or 1.5σ seems consistent to the experimental data [2], but the detailed comparison is difficult here due to



the treatment of the impact parameter determination.

IV. CALCULATED RESULTS OF FLOW

The collective transverse momentum flow is an observable quantity which reflects the interaction during the heavy ion collisions more sensitively than the quantity discussed in the previous section. In this paper, the flow is defined by

$$\langle wP_x/A \rangle = \frac{\sum_k A_k \text{sign}(P_{kz}) P_{kx}/A_k}{\sum_k A_k}, \quad (7)$$

where k is the index of the produced fragments in all events and A_k are their mass numbers. P_{kz} and P_{kx} are the components of the fragment momenta in the center-of-mass system along the beam direction and the transverse direction in the reaction plane respectively. The direction of x axis is taken so that the positive value of flow means repulsive flow. When summation is taken over all nucleons and fragments in Eq. (7), it means the inclusive flow. In the following we limit the summation to the fragments with a specific mass number and discuss the exclusive flow.

It is also possible to use the more commonly adopted definition of flow as the slope parameter of $\langle P_x/A \rangle$ - V_z curve [1,3]

$$\frac{V_P - V_T}{2} \left. \frac{d\langle P_x/A \rangle}{dV_z} \right|_{V_z=(V_P+V_T)/2}, \quad (8)$$

where V_P and V_T are the projectile and target velocities respectively. However it is more convenient in our numerical calculation to adopt the definition Eq. (7) because the statistical error is smaller than when Eq. (8) is adopted. Furthermore the flow $\langle wP_x/A \rangle$ in Eq. (7) is almost free from the ambiguity in the momentum width of the produced fragments in AMD simulations. We have checked in our previous work [9] that both definitions of the flow give similar results except for the difference in the absolute value.

In Fig. 4, we show the incident energy dependence of the calculated flows of nucleons and fragments with mass numbers $A = 1, 2, 3$ and 4 separately for $^{40}\text{Ar} + ^{27}\text{Al}$ collisions with the fixed impact parameter 3 fm. For the moment we concentrate on the results with Gogny force and the stochastic collision cross section 1.0σ , and the dependence on them will be discussed in a later section. As the incident energy increases from 25 MeV/nucleon to 135 MeV/nucleon, the flow changes from negative (attractive) value to the positive (repulsive) value at a certain incident energy called balance energy. The balance energy for nucleon flow is about 85 MeV/nucleon and the balance energy for fragments is higher than it. In the energy region where the flow is negative, the absolute value of the flow is larger for heavier fragment. The flow takes its minimum (namely the most attractive) value between 30 MeV/nucleon and 50 MeV/nucleon, and at 25 MeV/nucleon the absolute value of flow is small. This is evidently because of the almost spherical momentum distribution in fusion-like events. These qualitative features as well as the quantitative results are consistent to the experimental data in the energy region $25 \text{ MeV} \leq E/A \leq 85 \text{ MeV}$ where the data are available, as is shown in Fig. 5. The calculated flow in this figure is defined by Eq. (8) in the

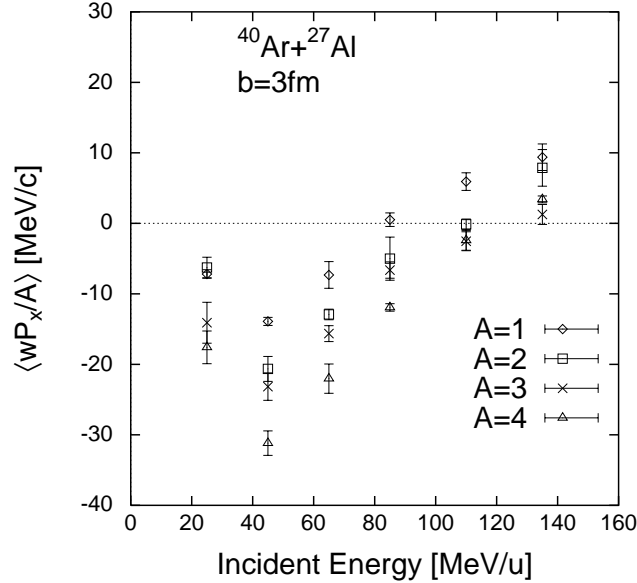


FIG. 4. Calculated results of the flow of nucleons and fragments with mass number $A = 1, 2, 3, 4$ in the $^{40}\text{Ar} + ^{27}\text{Al}$ collisions at various incident energies. The impact parameter is fixed to be 3 fm. Error bars show estimated statistical error of the calculation.

similar way to the experimental value. The experimental data are plotted in the positive side because there is no way to determine the sign of the flow only from the experiment, but evidently they should be considered to be negative at least in the energy region $E/A < 70$ MeV.

In order to clarify the origin of the calculated feature of the flow, especially the dependence of the flow on the particle mass number, we classify the particles according to the time they are produced in the calculation just as we have done in Ref. [9]. Figure 6 shows the flow of dynamically produced particles which existed at the end of the AMD calculation, namely at $t = t_{\text{sw}}$, and the flow of evaporated particles which are produced in the statistical decay process. As we have found in the previous work for $^{12}\text{C} + ^{12}\text{C}$ collisions [9], we can get the interpretation that there are two components of flow at the end of the dynamical stage of the reaction. The first component is the flow of dynamically emitted nucleons and the second component is the flow of excited fragments or the nuclear matter. In the energy region where the flow is negative, the absolute value of the first component is small because the nucleons are emitted by the stochastic two-nucleon collisions which erase the effect of the attractive mean field. The second component has larger absolute value in which large effect of the attractive interaction between projectile and target is remained. Also in higher energy region, the flow of dynamically emitted nucleons is more repulsive than the flow of excited fragments, which results in the difference of the balance energies of nucleons and fragments in the finally observed flow.

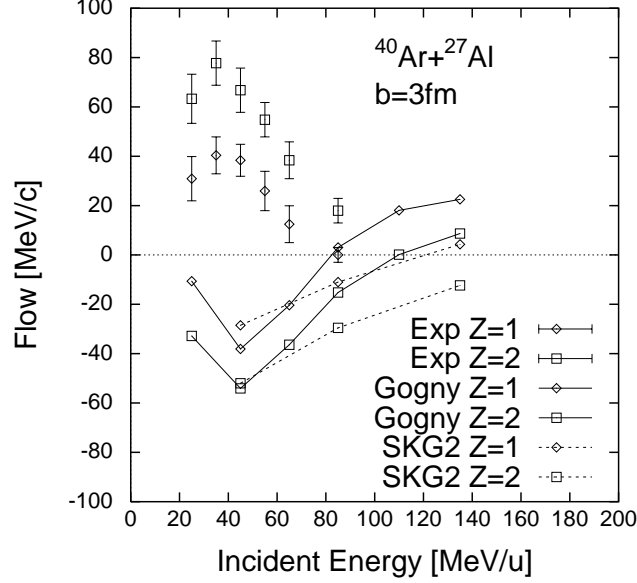


FIG. 5. Comparison of the calculated results with the experimental data [3]. Calculated flow in this figure is defined as the slope parameter of $\langle P_x/A \rangle - V_z$ curve in the similar way to Refs. [1,3]. Shown experimental data is the data in Fig. 3 of Ref. [3] multiplied by a factor introduced in Ref. [1] for the correction of the reaction plane determination. The experimental data are plotted in the positive side artificially.

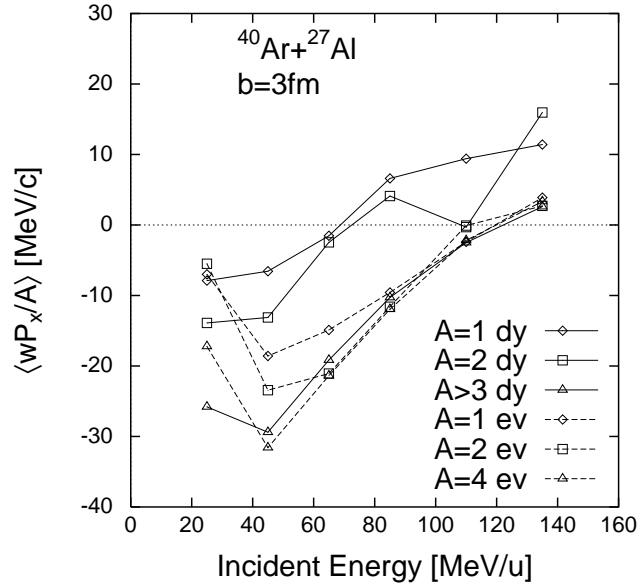


FIG. 6. The flows of dynamically produced particles which are calculated before the statistical decay process, and the flows of evaporated particles which are calculated only from the decay products of the statistical decay.

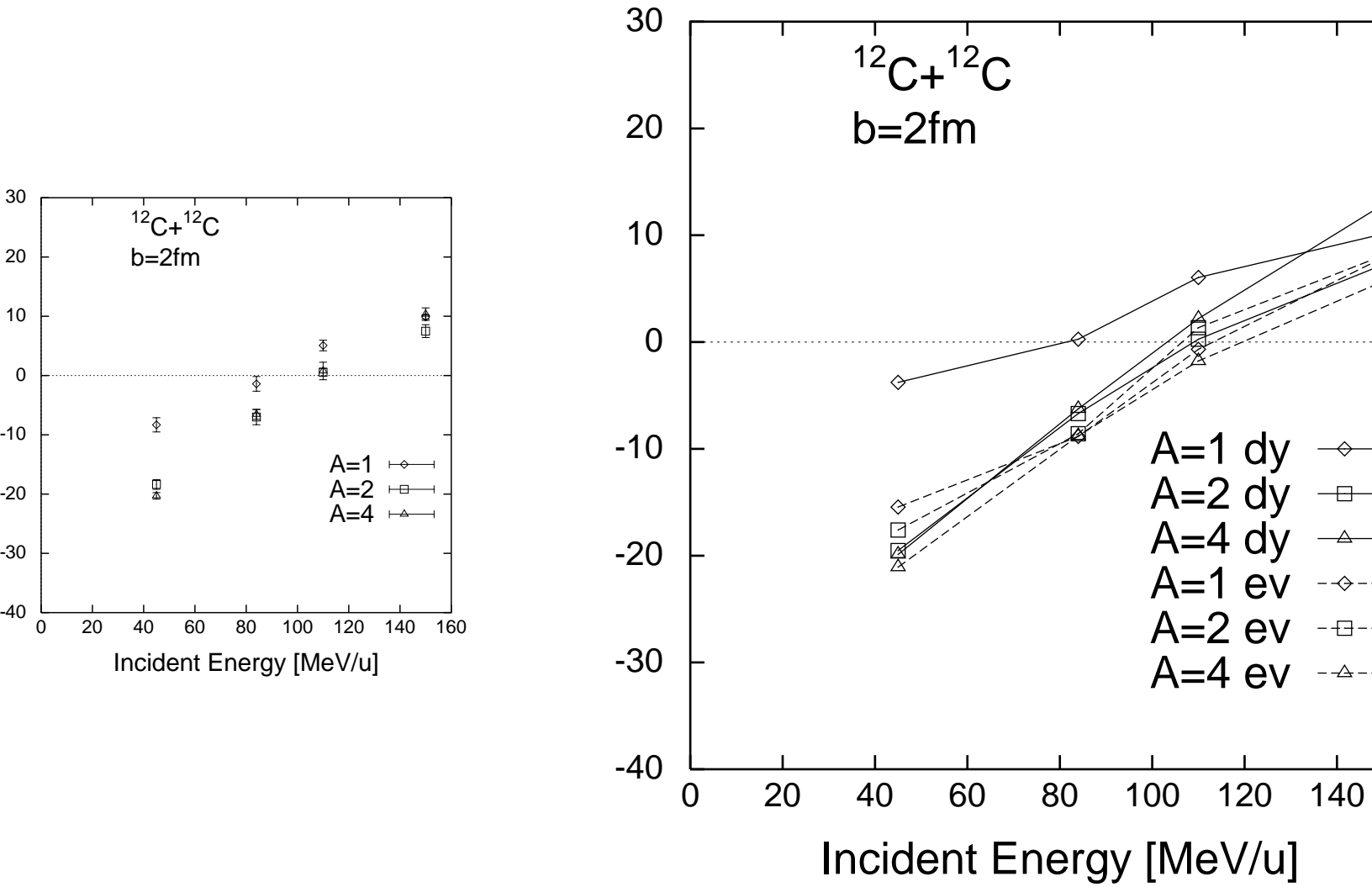


FIG. 7. Flow of nucleons, deuterons and α particles in $^{12}\text{C} + ^{12}\text{C}$ collisions with $b = 2\text{ fm}$ which was calculated in the work of Ref. [9].

TABLE IV. Comparison of the production mechanism of deuterons and α particles in $^{12}\text{C} + ^{12}\text{C}$ collisions (at 45 MeV/nucleon and 84 MeV/nucleon) and $^{40}\text{Ar} + ^{27}\text{Al}$ collisions (at 45 MeV/nucleon and 85 MeV/nucleon). See text for detail.

		45 MeV/nucleon		84–85 MeV/nucleon	
		C+C	Ar+Al	C+C	Ar+Al
d	M	0.50	0.57	1.04	0.86
	P_{PT}	$17 \pm 2\%$	$35 \pm 5\%$	$15 \pm 1\%$	$28 \pm 3\%$
α	M	1.29	0.12	1.12	0.12
	P_{PT}	$9 \pm 1\%$	$35 \pm 10\%$	$7 \pm 1\%$	$21 \pm 8\%$

V. PRODUCTION MECHANISM OF LIGHT FRAGMENTS AND THEIR FLOW

Although we have found many similarities between $^{40}\text{Ar} + ^{27}\text{Al}$ collisions with $b = 3$ fm and $^{12}\text{C} + ^{12}\text{C}$ collisions with $b = 2$ fm which we have studied in Ref. [9], there is an essential difference in the magnitude of the flow with respect to the fragment mass number. In $^{12}\text{C} + ^{12}\text{C}$ collisions the fragments with mass numbers $A \geq 2$ have almost an identical flow value as shown in Fig. 7. On the other hand in $^{40}\text{Ar} + ^{27}\text{Al}$ collisions, the flows of particles with mass numbers $A = 1, 2, 3$, and 4 are ordered according to their mass numbers as can be seen in Fig. 4. This feature is also observed in experiments of $^{40}\text{Ar} + ^{45}\text{Sc}$ collisions [4]. We have found here that this difference of flow comes from the difference of the flow behavior of dynamically produced deuterons while the flow of evaporated deuterons has similar value to the flow of excited fragments as shown in Fig. 6. The flow of dynamically produced deuterons has a value which is close to the flow of dynamical nucleons rather than the flow of heavier fragments in $^{40}\text{Ar} + ^{27}\text{Al}$ collisions, while there is no difference between deuteron flow and flow of heavier fragments in $^{12}\text{C} + ^{12}\text{C}$ collisions as seen in Fig. 7.

The origin of this different flow behavior of the dynamically produced deuterons in $^{12}\text{C} + ^{12}\text{C}$ collisions and $^{40}\text{Ar} + ^{27}\text{Al}$ collisions can be understood in the following way by paying attention to the production mechanism of deuterons. We have traced back the proton and the neutron of each dynamically produced deuteron in the calculation and checked whether they originate from different initial nuclei (i.e., one from the projectile and the other from the target) or they come from the same nucleus (i.e., both from the projectile or both from the target). The former probability is denoted by P_{PT} and the latter probability is therefore $1 - P_{PT}$. The calculated values of P_{PT} are shown in Table IV together with the multiplicities M of deuterons and α particles. For α particles, P_{PT} is defined as the probability that the α particle contains at least one nucleon from the projectile and at least one nucleon from the target. In $^{12}\text{C} + ^{12}\text{C}$ collisions only 15% of dynamically produced deuterons are composed of two nucleons from different nuclei, while this ratio is about 30% in $^{40}\text{Ar} + ^{27}\text{Al}$ collisions. With respect to P_{PT} , no significant difference greater than the statistical error has been obtained between 45 MeV/nucleon and 85 MeV/nucleon. Such deuterons should have been produced by the coalescence, i.e., two nucleons which are emitted by stochastic collisions have merged and formed deuterons when they happened to be close in the phase space. It should be noted that the P_{PT} is at most about 50% even if all deuterons are created by the coalescence because two nucleons from the same nucleus can form a deuteron by

the coalescence with the similar probability to the two nucleons from different nuclei. In other words, $P_{PT} = 15\%$ in $^{12}\text{C} + ^{12}\text{C}$ collisions means that about 30% of the dynamically produced deuterons have been produced by the coalescence, and other 70% of dynamical deuterons are produced by other mechanisms with which only the nucleons from the same nucleus can form a deuteron. In the latter mechanisms, of course, the two nucleons have not suffered the direct effect of the stochastic collisions. In the case of $^{40}\text{Ar} + ^{27}\text{Al}$ collisions, $P_{PT} = 30\%$ means that the coalescence mechanism occupies about 60% of the total deuterons produced dynamically. Strictly speaking, we should take account of the mass asymmetry of the projectile and the target in the above discussion, but this effect can be easily shown to be negligible in the case of $^{40}\text{Ar} + ^{27}\text{Al}$ collisions.

Thus there is large dependence of the production mechanism of dynamical deuterons on the mass number of the system. This fact can explain the difference of the deuteron flow between these reactions. The deuterons created by the coalescence should reflect the momenta of the nucleons which have been emitted by the stochastic collisions and have happened to compose the deuterons, and therefore the flow of such deuterons should have the flow similar to that of dynamically emitted nucleons. This is the origin of the dynamical deuteron flow which is close to the dynamical nucleon flow in $^{40}\text{Ar} + ^{27}\text{Al}$ collisions as shown in Fig. 6. On the other hand, the dynamical deuteron flow is the same as the flow of excited fragments in $^{12}\text{C} + ^{12}\text{C}$ collisions because most deuterons are created without the direct effect of the stochastic collisions.

In Table IV, we can also find the significant difference in the production mechanism of the dynamical α particles. There is a large difference in the calculated multiplicity, the origin of which is the difference in the yield of α particles composed of four nucleons from the same nucleus. In $^{12}\text{C} + ^{12}\text{C}$ collisions, P_{PT} is quite small and the multiplicity of α particles which are produced without direct effect of stochastic collisions is about 1, which is larger by an order of magnitude than in $^{40}\text{Ar} + ^{27}\text{Al}$ collisions.

VI. DEPENDENCE OF THE FLOW ON σ AND EOS

Although the ultimate purpose of the study of the flow is to determine the EOS of the nuclear matter, we should also study the dependence of the flow on the stochastic collision cross section (σ) at the same time since there is much theoretical ambiguity in the adopted stochastic collision cross section. Of course it is more desirable to fix σ by studying other quantities, such as the momentum distribution of fragments discussed in Sec. III, and comparing them to the experimental data. However, we will see in this section fortunately that the study of the flow of nucleons and fragments gives us much information on the EOS in spite of the uncertainty of σ .

In Fig. 8, the flow of nucleons and α particles are shown for the calculation with the standard cross section 1.0σ (symbols connected with solid lines) and increased cross section 1.5σ (pluses and crosses without lines). Figs. 9 and 10 show the deformation parameter β_{flow} and the flow angle Θ_{flow} of the kinetic flow tensor

$$F_{ij} = \frac{\sum_k P_{ki} P_{kj} / A_k}{\sum_k A_k}, \quad (9)$$

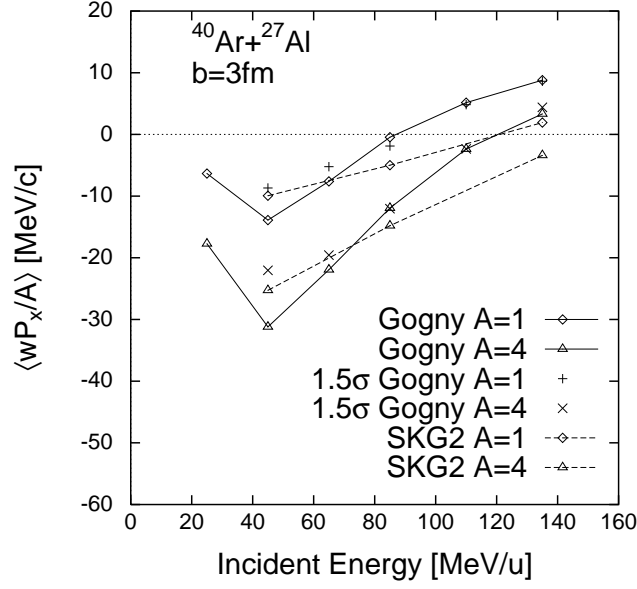


FIG. 8. Nucleon flow and α flow in $^{40}\text{Ar} + ^{27}\text{Al}$ collisions with $b = 3\text{ fm}$. Calculated results with Gogny force (solid line) and with SKG2 force (dashed line) are shown as well as the results with Gogny force and increased cross section 1.5σ (pluses and crosses without line).

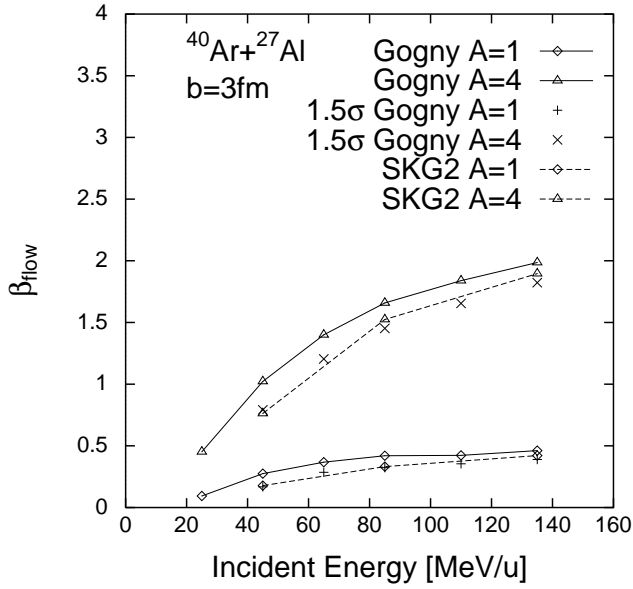


FIG. 9. The quadrupole deformation parameter of the flow tensor.

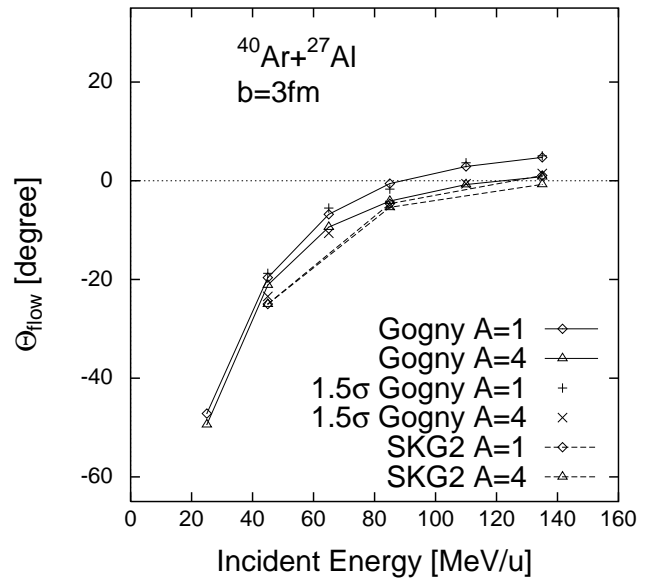


FIG. 10. The calculated value of the flow angle.

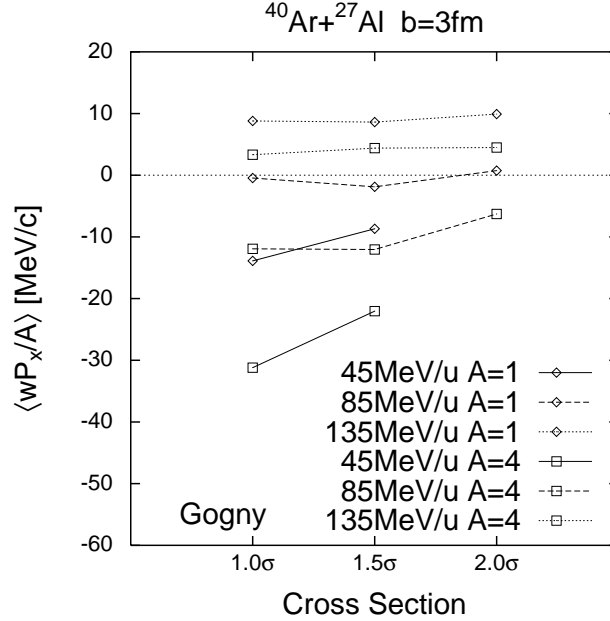


FIG. 11. The σ -dependence of the nucleon flow and the α flow in $^{40}\text{Ar} + ^{27}\text{Al}$ collisions with $b = 3$ fm in the calculation with the Gogny force.

where k is the index of the produced fragments in all events and $i, j = x, y, z$. The summation is limited to the fragments with a given mass number in Figs. 9 and 10. The flow angle Θ_{flow} is the angle between the beam direction and the eigenvector of F_{ij} corresponding to the largest eigenvalue. Negative Θ_{flow} means the attractive flow. Denoting the ratio of eigenvalues of F_{ij} as $e^{2t_1} : e^{2t_2} : e^{2t_3}$ with $t_1 + t_2 + t_3 = 0$ and $t_1 \leq t_2 \leq t_3$, we define the deformation parameter β_{flow} in the similar way to Eq. (6). The parameter β_{flow} represents the degree of the dissipation of the incident energy which can be also shown by the parallel momentum distribution like in Fig. 3. Smaller β_{flow} means larger dissipation. In relatively low energy region $E/A \sim 45$ MeV/nucleon, the flow has large dependence on the stochastic collision cross section as can be seen from Fig. 8. For larger σ the absolute value of the flow is smaller. As we have found in our previous work [9], this decrease of the flow comes from the increase of the dissipated components in the momentum distribution, which has appeared as the decrease of β_{flow} in Fig. 9. Note that Θ_{flow} is not sensitive to σ because the spherical dissipated component does not affect the eigenvectors of F_{ij} . The flow angle of α particles increases slightly according to the increase of σ , but the decrease of β_{flow} is much larger and, as the result, the value of the flow decreases. The flow angle Θ_{flow} is also insensitive to the mass number of the fragment, which is also an expected result from the interpretation of the two component of flow. Namely, the eigenvectors of nucleon flow tensor is essentially decided by the flow of the evaporated nucleons which is identical to the flow of the excited fragments, because the almost spherical component of dynamically emitted nucleons does not affect them. Therefore if the independence of the flow angle is observed in experiment, it will be a strong evidence of the two component of the flow in this energy region.

In higher energy region $E/A \gtrsim 85$ MeV, on the other hand, the σ -dependence of the flow

is quite small in our calculation. The multiplicity of nucleons changes sensitively to σ and the dissipation increases to some degree for larger σ as shown in Fig. 9. However the change of the β_{flow} is small compared to the absolute value of the deformation parameter β_{flow} . The flow angle Θ_{flow} , and therefore the value of flow, do not change at all. When the cross section is further increased up to 2.0σ , a little σ -dependence is found at 85 MeV/nucleon especially in the flow of α particles, as shown in Fig. 11, because the dissipation becomes rather large. At 135 MeV/nucleon, however, the σ -dependence is quite small in the wide region between 1.0σ and 2.0σ .

Not only with Gogny force which corresponds to the incompressibility of the nuclear matter $K = 228$ MeV, we have also made calculations with the SKG2 force. The SKG2 force corresponds to the large incompressibility $K = 373$ MeV and the mean field has no momentum dependence. The results with SKG2 force have been shown in Figs. 8, 9, 10 and 5 by dashed lines.

As is evident from these figures, the calculated flow with SKG2 force does not reproduce the data of Refs. [1,3] in two points. Firstly, the balance energy is too large even with this effective interaction which corresponds to the stiff EOS. Secondly, the incident energy dependence of the flow of nucleons and fragments is much smaller than with the Gogny force. The calculated results suggest that the momentum dependence of the mean field is more important than the density dependence in order to reproduce the large incident energy dependence and the small balance energy. Since the σ -dependence of these features is small as we have discussed above, we can conclude that the SKG2 force, i.e., the stiff EOS without momentum dependence of the mean field is inconsistent to the observed data of the flow of nucleons and fragments in the intermediate energy region, while the Gogny force, which corresponds to the soft EOS with momentum dependence of the mean field, reproduce the data very well.

Finally, we notice that the dissipation or the stopping is larger with the SKG2 force than with the Gogny force when the same stochastic collision cross section 1.0σ is adopted, as can be seen in Fig. 9. In order to see whether this feature is really due to the effect of the mean field, we calculated the trajectory of the projectile and the target without any stochastic collisions at the incident energy 45 MeV/nucleon and with the impact parameter 3 fm. Figure 12 shows the time development of the absolute value and the x component of the relative velocity of the target and the projectile for 8 events. The difference among events is due to the random orientation of the initial nuclei. The velocity of the projectile (the target) is calculated from the time development of the center-of-mass of the physical positions $\{\text{Re } \mathbf{W}_i\}$ defined by Eq. (4) which originate from the projectile (the target). It is clearly seen that the acceleration due to the attractive mean field is suppressed with the SKG2 force compared to the calculation with the Gogny force, probably due to the large incompressibility of the SKG2 force [18]. As the result, with the SKG2 force, the interaction time is longer and the one-body dissipation of the incident velocity is larger. The final transverse relative velocity is larger with the SKG2 force, which is in accordance with the larger flow angle in Fig. 10 in the calculation with stochastic collisions.

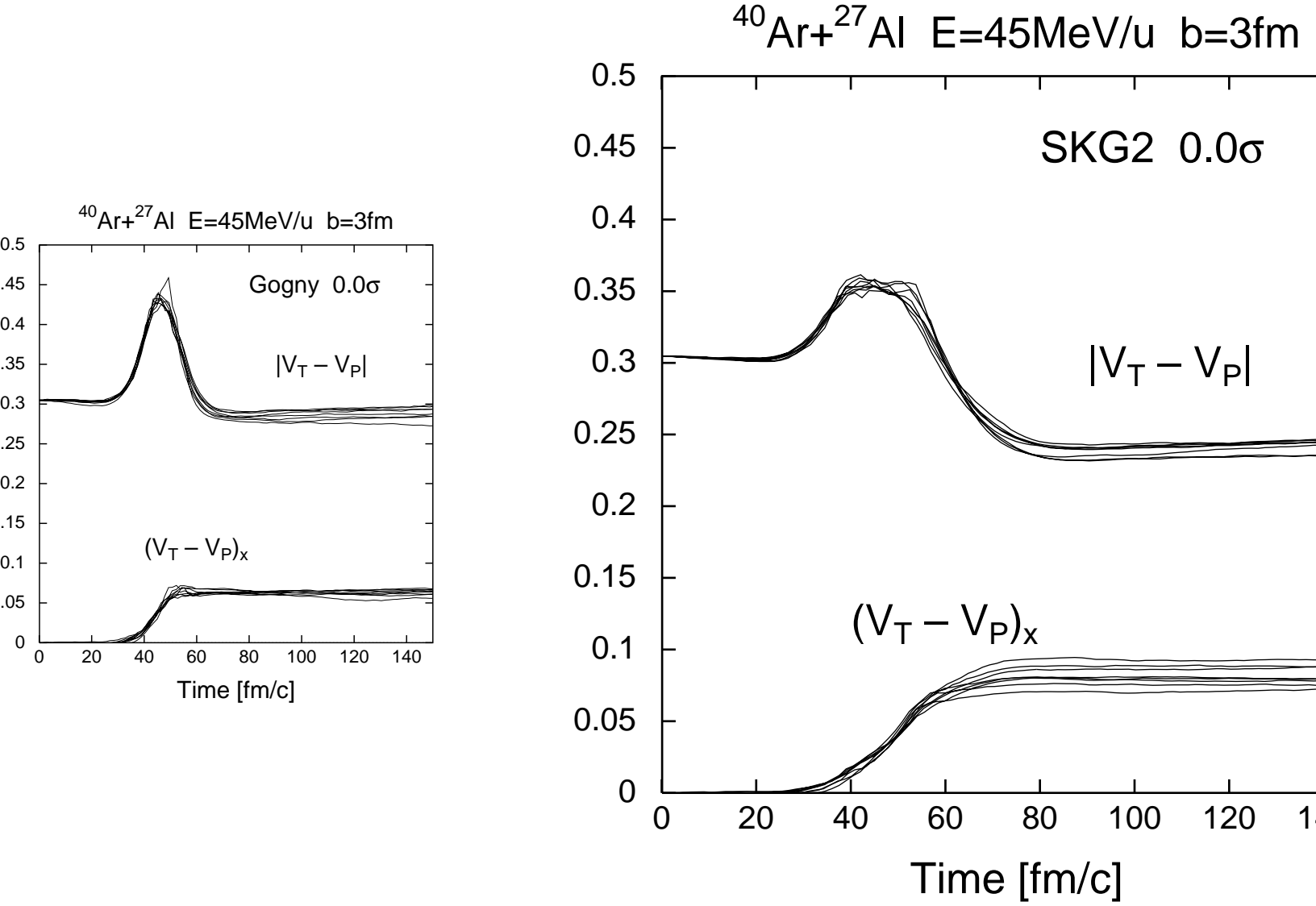


FIG. 12. The time development of the relative velocity of the target and the projectile $\mathbf{V}_T - \mathbf{V}_P$ in the calculation without stochastic collisions. Its absolute value and its x component in 8 events at 45 MeV/nucleon are shown for the Gogny force (left) and the SKG2 force (right).

VII. SUMMARY

In this paper, we studied $^{40}\text{Ar} + ^{27}\text{Al}$ collisions with AMD in the incident energy region $25 \text{ MeV} \leq E/A \leq 135 \text{ MeV}$, aiming to study the exclusive flow of nucleons and fragments and to determine the EOS of the nuclear matter. The impact parameter was fixed to 3 fm in most cases. The calculations were performed with two effective interactions, namely the Gogny force which corresponds to the soft EOS with reliable momentum dependence of the mean field and the SKG2 force which corresponds to the stiff EOS without momentum dependence of the mean field. The calculation with the Gogny force reproduced quite successfully many features of the experimental data of the flow of nucleons and fragments, such as the balance energy, the absolute value and the incident energy dependence of the flow, and the large fragment flow compared to the nucleon flow. Such features were explained by the concept of the two components of the flow, i.e., the dynamical nucleon flow and the flow of excited fragments at the end of the dynamical stage of the reaction.

On the other hand, the calculation with the SKG2 force failed in reproducing the data. The calculated balance energy is too large and the incident energy dependence of the flow is too small. We also checked the dependence of the flow on the stochastic collision cross section and found that there is some σ -dependence in the energy region $E/A \sim 45 \text{ MeV}$ which can be related to the dissipated component in the momentum distribution but the σ -dependence is quite small in the energy region $E/A \gtrsim 85 \text{ MeV}$. Therefore, even if the theoretical ambiguity of the stochastic collision cross section in the nuclear medium is taken into account, we can conclude that the stiff EOS without the momentum dependence is inconsistent to the observed data, while the data are well reproduced with the Gogny force which gives a soft EOS with the momentum dependent mean field.

Our calculated results on the EOS dependence of the balance energy is similar to the results of QMD by Ohnishi et al. [19] where the statistical decay process was not taken into account. However, our calculated σ -dependence is different from their results.

We also compared the calculated results with the results for $^{12}\text{C} + ^{12}\text{C}$ collisions studied in our previous work [9]. In addition to many similarities concerned with the flow of nucleons and fragments, we found a significant difference in the flow of dynamically produced deuterons. In $^{12}\text{C} + ^{12}\text{C}$ collisions, most dynamical deuterons are produced without direct effect of the stochastic collisions and their flow is identical to the flow of excited fragments. On the other hand in $^{40}\text{Ar} + ^{27}\text{Al}$, many dynamical deuterons are created by the coalescence of the nucleons which are emitted by the stochastic collisions, and therefore the flow of dynamical deuterons is close to the flow of dynamical nucleons. In the production mechanism of α particles, similar difference were found between $^{12}\text{C} + ^{12}\text{C}$ collisions and $^{40}\text{Ar} + ^{27}\text{Al}$ collisions.

ACKNOWLEDGMENTS

The computational calculation for this work was partly supported by Research Center for Nuclear Physics, Osaka University, as an RCNP Computational Nuclear Physics Project (Project No. 92-B-04). Other part of the computational calculation was performed on the

super computer FACOM VPP-500 in RIKEN. One of the authors (A. O.) is supported by JSPS fellowship.

REFERENCES

- [1] J. Péter, in *Proc. Int. Symp. on Heavy Ion Physics and Its Application, Lanzhou, 1990*, edited by W. Q. Shen et al., (World Scientific, Singapore, 1991), p.191.
- [2] J. Péter, J. P. Sullivan, D. Cussol, G. Bizard, R. Brou, M. Louvel, J. P. Patry, R. Regimbart, J. C. Steckmeyer, B. Tamain, E. Crema, H. Doubre, K. Hagel, G. M. Jin, A. Péghaire, F. Saint-Laurent, Y. Cassagnou, R. Legrain, C. Lebrun, E. Rosato, R. MacGrath, S. C. Jeong, S. M. Lee, Y. Nagashima, T. Nakagawa, M. Ogihara, J. Kasagi and T. Motobayashi, *Phys. Lett.* **B237**, 187 (1990).
- [3] J. P. Sullivan, J. Péter, D. Cussol, G. Bizard, R. Brou, M. Louvel, J. P. Patry, R. Regimbart, J. C. Steckmeyer, B. Tamain, E. Crema, H. Doubre, K. Hagel, G.M. Jin, A. Péghaire, F. Saint-Laurent, Y. Cassagnou, R. Legrain, C. Lebrun, E. Rosato, R. MacGrath, S. C. Jeong, S. M. Lee, Y. Nagashima, T. Nakagawa, M. Ogihara, J. Kasagi and T. Motobayashi, *Phys. Lett.* **B249**, 8 (1990).
- [4] G. D. Westfall, W. Bauer, D. Craig, M. Cronqvist, E. Gualtieri, S. Hannuschke, D. Klakow, T. Li, T. Reposeur, A. M. Vander Molen, W. K. Wilson, J. S. Winfield, J. Yee, S. J. Yennello, R. Lacey, A. Elmaani, J. Lauret, A. Nadasen, and E. Norbeck, *Phys. Rev. Lett.* **71**, 1986 (1993).
- [5] K. G. R. Doss, H.-A. Gustafsson, H. Gutbrod, J. W. Harris, B. V. Jacak, K.-H. Kampert, B. Kolb, A. M. Poskanzer, H.-G. Ritter, H. R. Schmidt, L. Teitelbaum, M. Tincknell, S. Weiss and H. Wieman, *Phys. Rev. Lett.* **59**, 2720 (1987).
- [6] A. Ono, H. Horiuchi, Toshiki Maruyama and A. Ohnishi, *Phys. Rev. Lett.* **68**, 2898 (1992).
- [7] A. Ono, H. Horiuchi, Toshiki Maruyama and A. Ohnishi, *Prog. Theor. Phys.* **87**, 1185 (1992).
- [8] A. Ono, H. Horiuchi, Toshiki Maruyama and A. Ohnishi, *Phys. Rev.* **C47**, 2652 (1993).
- [9] A. Ono, H. Horiuchi and Toshishi Maruyama, *Phys. Rev.* **C48**, 2946 (1994).
- [10] H. Feldmeier, *Nucl. Phys.* **A515**, 147 (1990).
- [11] H. Horiuchi, *Nucl. Phys.* **A522**, 257c (1991).
- [12] H. Horiuchi, T. Maruyama, A. Ohnishi, and S. Yamaguchi, in *Proc. Int. Conf. on Nuclear and Atomic Clusters, Turku, 1991*, edited by M. Brenner, T. Lönnroth and F. B. Malik, (Springer, Berlin, 1992), p.512; in *Proc. Int. Symp. on Structure and Reactions of Unstable Nuclei, Niigata, 1991*, edited by K. Ikeda and Y. Suzuki, (World Scientific, Singapore, 1992), p.108.
- [13] J. Dechargé and D. Gogny, *Phys. Rev.* **C43**, 1568 (1980).
- [14] A. Ohnishi, H. Horiuchi and T. Wada, *Phys. Rev.* **C41**, 2147 (1990).
- [15] T. Maruyama, A. Ono, A. Ohnishi and H. Horiuchi, *Prog. Theor. Phys.* **87**, 1367 (1992).
- [16] F. Pühlhofer, *Nucl. Phys.* **A280**, 267 (1977).
- [17] R. Dayras, A. Pagano, J. Barrette, B. Berthier, D. M. De Castro Rizzo, E. Chavez, O. Cisse, R. Legrain, M. C. Mermaz and E. C. Pollacco, *Nucl. Phys.* **A460**, 299 (1986).
- [18] T. Wada, S. Yamaguchi and H. Horiuchi, *Phys. Rev.* **C41**, 160 (1990).
- [19] A. Ohnishi, T. Maruyama and H. Horiuchi, in *Proc. Tours Symp. on Nuclear Physics, Tours, 1991*, edited by M. Ohta and B. Remaud, (World Scientific, Singapore, 1992), p.110.